

Seasonal Monitoring and Analysis of Soil Moisture and Vegetation Health in Oil Palm Plantations Using Remote Sensing

Ismail, S. I.,¹ Ya'acob, N. S.,^{1,2*} Kassim, M.,^{1,3} and Nik Dzulkefli, N. N. S.¹

¹School of Electrical Engineering, College of Engineering, Universiti Teknologi MARA, 40450 Shah Alam, Selangor, Malaysia, E-mail: norsuzila@uitm.edu.my*

²Wireless Communication Technology (WiCoT), College of Engineering, Universiti Teknologi MARA, 40450 Shah Alam, Selangor, Malaysia

³Institute for Big Data Analytics and Artificial Intelligence (IBDAAI), Kompleks Al-Khwarizmi, Universiti Teknologi MARA, 40450 Shah Alam, Selangor, Malaysia

*Corresponding Author

DOI: <https://doi.org/10.52939/ijg.v21i4.4069>

Abstract

Malaysia, a prominent producer of palm oil in Asia, faces the challenge of regulating plantations to ensure optimal productivity. Manual monitoring proves impractical due to the associated energy, expense, and time constraints. Consequently, cost-effective, and time-saving alternatives such as remote sensing (RS) and Geographic Information System (GIS) utilizing satellite imagery become crucial for palm oil monitoring. These technologies leverage spectral and texture studies for vegetation classification. This study integrates remote sensing techniques to assess soil moisture dynamics and vegetation health in oil palm plantations, aiming to enhance sustainable agricultural management practices. The research utilizes the Soil Moisture Index (SMI) and Normalised Difference Vegetation Index (NDVI), derived from Landsat 9 satellite imagery accessed and processed using Climate Engine and ArcGIS Pro software, to analyze seasonal variations and their implications. Key findings reveal distinct seasonal patterns: high soil moisture levels during wet periods (SMI Level 5) support optimal vegetation health (NDVI Level 3) and face challenges of waterlogging, contrasted with low soil moisture during dry seasons (SMI Level 1), requiring adaptive irrigation strategies to maintain vegetation health. Correlation analysis underscores the significant relationship between soil moisture, vegetation health, and climatic variables (temperature, precipitation), guiding the development of targeted management strategies. This research contributes novel insights into the integrated use of SMI and NDVI for agricultural sustainability, offering practical implications for adaptive management and resource optimization in oil palm plantations, such as developing irrigation schedules and drainage systems tailored to seasonal conditions.

Keywords: Climate, Oil Palm Plantation, Remote Sensing, Normalised Difference Vegetation Index, Soil Moisture Index

1. Introduction

Oil palm plantations are economically significant as they are a major source of vegetable oil globally, supporting millions of livelihoods. Ecologically, these plantations can impact local biodiversity and soil health, making sustainable management practices essential. Effective management of oil palm plantations is crucial for maintaining productivity and sustainability. Traditional methods of monitoring soil moisture and vegetation health are often labor-intensive and time-consuming. In recent years, remote sensing technologies have emerged as vital tools for monitoring agricultural landscapes, offering a more efficient and cost-effective alternative

[1][2][3][4] and [5]. These technologies enable the collection of data over large areas at various temporal and spatial scales, allowing for detailed analysis of seasonal changes in soil moisture and vegetation health.

Soil moisture and vegetation indices are critical indicators of agricultural health and productivity, especially in regions dominated by cash crops such as oil palm plantations. *Normalised Difference Vegetation Index (NDVI)* and *Soil Moisture Index (SMI)* are widely used in remote sensing to monitor vegetation cover and soil moisture, respectively.

Understanding the relationship between these indices and climate factors such as temperature and precipitation is crucial for effective plantation management and predicting crop performance under varying climatic conditions. The significance of this relationship lies in its potential to enhance irrigation practices, optimize fertilizer use, and mitigate the impacts of climate change on crop yield and soil health.

Remote sensing technologies enable continuous monitoring over different seasons, providing insights into how seasonal changes, particularly the dry and monsoon seasons characterized by variations in temperature and precipitation, affect soil moisture and vegetation health. Mapping *NDVI* and *SMI* during these seasons allows for a comprehensive health assessment of the oil palm trees, identifying stress factors and areas needing attention [6] and [7]. For example, remote sensing can detect variations in soil moisture levels that might indicate irrigation needs or potential water stress areas [8][9] and [10]. This early detection allows plantation managers to implement targeted interventions, thereby improving water use efficiency and reducing the risk of crop failure.

Remote sensing provides a suite of tools, including satellite imagery and aerial photography, which can capture a wide range of spectral information. Specific remote sensing techniques such as Landsat 8 imagery, Sentinel-2, and MODIS provide valuable spectral information for calculating indices like *NDVI* and *SMI*. These techniques use optical and thermal infrared sensors to capture data relevant to vegetation health and soil moisture levels. This information is essential for understanding the health and status of vegetation [11][12] and [13]. For instance, indices such as the *Normalised Difference Vegetation Index (NDVI)* can be used to assess plant health, especially in areas with varying soil backgrounds, while the *Soil Moisture Index (SMI)* helps in understanding the soil moisture levels critical for the growth of oil palm trees. By leveraging remote sensing data, it is possible to assess the impacts of environmental factors and management practices on oil palm plantations, facilitating timely decision-making to optimize crop yields and resource use.

Seasonal weather changes significantly influence vegetation and soil moisture dynamics. Soil moisture plays a critical role in vegetation phenology, particularly in water-limited regions where temperature and soil moisture are key factors affecting the start and end of the growing season [14]. Seasonal changes in forest ecosystems can alter soil hydraulic properties, impacting soil moisture dynamics. Variations in soil hydraulic parameters are

closely related to changes in leaf area index, litterfall, and heterotrophic respiration [15]. During the peak growing season, global interactions between soil moisture and climate factors reveal positive relationships with precipitation and evapotranspiration, and negative associations with temperature. This highlights the compounding effects of climate factors on soil moisture dynamics [16]. In seasonally dry tropical forests, changes in precipitation patterns significantly impact soil respiration and ecosystem components. Delayed and increased monsoon seasons lead to varying effects on soil moisture and vegetation indices [17][18] and [19]. Additionally, soil moisture levels are crucial for the stability and repeatability of spectral index values in geological remote sensing, emphasizing the need for data collection under optimal soil moisture conditions for accurate measurements [20].

The relationship between soil moisture index and plant health is pivotal for understanding vegetation growth and stress levels. Soil moisture index, derived from remote sensing data, is a significant tool for assessing plant water stress and overall health [7][21] and [22]. Monitoring soil moisture levels is essential for predicting drought stress, as insufficient soil moisture inhibits plant growth and can cause damage [23]. Soil moisture content can be estimated using remote sensing technologies like *NDVI* and interpolation methods, with interpolation being recommended for mapping soil water content in oil palm plantations [24]. The *Normalised Difference Vegetation Index (NDVI)*, derived from satellite data, has shown significant correlations with soil moisture, influencing crop health indicators in regions like Nebraska [25]. Studies utilizing spectral indices like *NDVI*, and *Normalised Difference Water Index (NDWI)* have demonstrated the relationship between soil moisture and vegetation health, particularly in analyzing the impact of heatwaves on vegetation in regions like Panjab, Haryana, and Rajasthan [26]. Synthetic Aperture Radar (SAR) data has proven effective in retrieving soil moisture content, with SAR-derived indicators like *Radar Vegetation Index (RVI)* showing promising accuracy in assessing soil moisture levels in oil palm crops [27] and [28]. Moreover, detecting diseases such as Basal Stem Rot (BSR) in oil palm trees has been linked to soil resistivity measurements. Healthy trees exhibit higher electrical resistance readings compared to infected ones, underscoring the importance of soil properties in plant health assessment [27]. The application of soil moisture indices in different agricultural settings has proven effective in monitoring plant health and guiding irrigation practices [29].

Additionally, studies have highlighted the significant role of soil moisture in determining oil palm productivity and health, emphasizing the need for continuous monitoring and management [30] and [31]. Despite the recognized importance of *NDVI* and *SMI* in agricultural monitoring, there is a lack of comprehensive studies that explore their relationship with climate factors in oil palm plantations. Previous research has largely focused on either soil moisture or vegetation indices independently, without integrating these parameters to understand their combined impact on crop performance. Additionally, there is limited research examining how these indices vary across different climatic conditions, particularly during the wettest and driest months. This gap in the literature underscores the need for an in-depth analysis to provide valuable insights for sustainable plantation management.

The objective of this study is to leverage remote sensing technology to monitor and analyze seasonal variations in soil moisture and vegetation health within oil palm plantations, thereby providing valuable insights for sustainable management practices. By integrating satellite data with climate factors, the research aims to enhance our understanding of how various environmental factors and management strategies influence plantation health and productivity over time. Specifically, this study seeks to explore the correlation between the *Normalised Difference Vegetation Index (NDVI)*, *Soil Moisture Index (SMI)*, and climate variables such as *temperature* and *precipitation* during the wettest

and driest months. The key aims are to identify the spatial and temporal variations of *NDVI* and *SMI* in response to different climate conditions and evaluate the impact of temperature and precipitation on *NDVI* and *SMI* within the context of oil palm plantations. In this research, remote sensing data from satellites such as Landsat 9 were utilized to calculate *NDVI* and *SMI* for the selected wettest and driest months. The analysis involved the correlation of these indices with temperature and precipitation data obtained from Climate Engine. ArcGIS Pro Software was used for mapping and spatial analysis. This research was expected to contribute to the field of agricultural monitoring by providing insights into the relationship between soil moisture, vegetation health, and climate factors. The findings were anticipated to aid in the development of more effective management practices for oil palm plantations, enhancing productivity and sustainability. Furthermore, the study demonstrated the utility of remote sensing technologies in agricultural research, potentially guiding future studies in similar contexts.

2. Material and Method

2.1 Study Area

Figure 1 shows a map of plantation, which spans 260 hectares and consists of four blocks: B36, B37, B38, and B39. The geographical coordinates of the study area are 4°03'31.49" N latitude and 103°13'33.18" E longitude. The area of each block is detailed in Table 1.

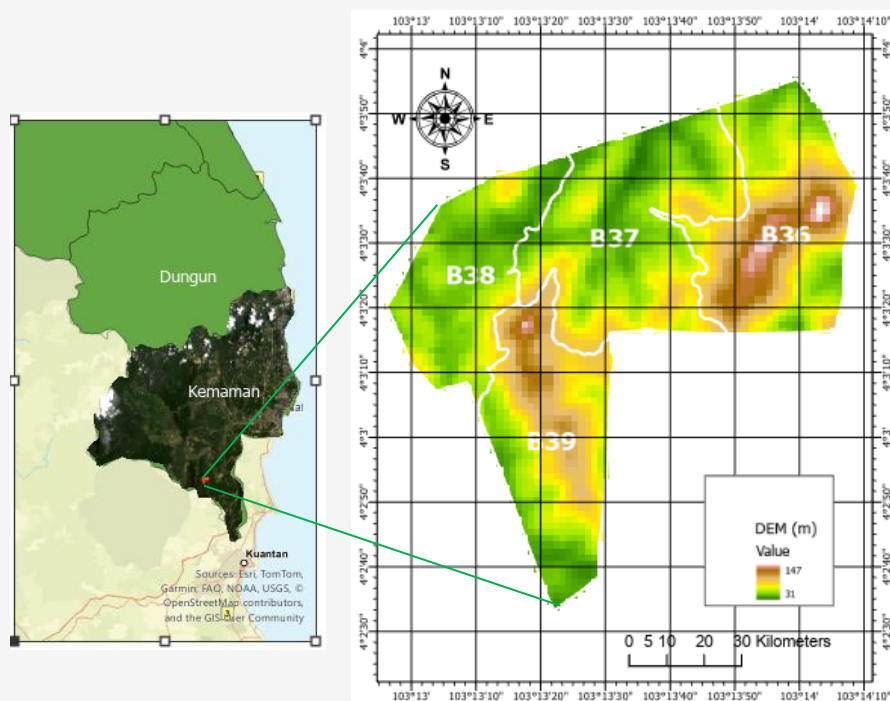


Figure 1: Study area of Felda Cherul Plantation - PM05Q division map

Table 1: The area of each block in the PM05Q division of the Felda Cheral plantation

Block	Area (hectares)
B36	67.59
B37	80.17
B38	50.47
B39	61.80
Total area	260.00

2.2 Satellite Image

To obtain high-quality satellite images with minimal cloud coverage, the Climate Engine platform can be utilized. Climate Engine provides access to pre-processed satellite data, enabling efficient data retrieval and analysis. The process begins by selecting the desired dataset, such as Landsat 9, and specifying the study area's coordinates along with the required date range. This ensures that the data corresponds to the relevant period and location. Climate Engine offers built-in cloud filtering techniques that automatically exclude cloud-contaminated pixels using quality assessment bands, ensuring only reliable data is used for analysis. The platform provides the option to compute vegetation indices such as *NDVI*, along with climate variables like precipitation and temperature, directly from the selected dataset. Once the parameters are set, the data is processed and visualized through an interactive interface, allowing for trend analysis and time-series exploration. The processed data can then be exported in various formats, such as CSV or GeoTIFF, for further analysis in ArcGIS Pro software. This streamlined approach helps in obtaining accurate and cloud-free satellite observations, facilitating effective monitoring of soil moisture and vegetation health in oil palm plantations.

2.3 Research Framework

The flowchart in Figure 2 used for analyzing the relationship between vegetation and soil moisture indices due to seasonal impacts began with defining study objectives and parameters. It moved on to data collection, acquiring satellite imagery and meteorological data. The data was then preprocessed, including atmospheric corrections and normalization for satellite images and organization of meteorological data. Vegetation and soil moisture indices (*SAVI*, and *SMI*) were calculated. Seasonal analysis was conducted by selecting representative months and calculating indices for these periods. The data was then analyzed and interpreted through temporal, spatial, and correlation analyses to understand relationships and seasonal variations. Finally, the results were visualized using graphs,

charts, and maps to present the findings. Heatmaps were generated to visualize the distribution of *Normalised Difference Vegetation Index (NDVI)* and *Soil Moisture Index (SMI)* levels across different blocks (B36, B37, B38, B39) and months (January, July, August, December). These heatmaps provide a clear and concise overview of vegetation health and soil moisture variations, facilitating a more comprehensive analysis

2.4 Climatology Temperature-Precipitation

Climatology, the study of climate, used data on precipitation and temperature to find long-term climate patterns. Precipitation and temperature were important because they greatly affected the growth of oil palm trees. By studying these factors, the aim was to understand the best conditions for oil palm cultivation and predict future climate changes that might impact its growth. Both the temperature and precipitation datasets were downloaded from Terra Climate, a high-resolution climate data source that provided detailed monthly climate and hydrology data. Terra Climate integrated information from satellites, weather stations, and climate models to offer comprehensive climate data from 1958 to the present. For this study, data was gathered from Terra Climate at a 4 km resolution, covering the period from January 2014 to December 2022, providing nine years of data. The data can be accessed at the following URL: <https://app.climateengine.org/climateEngine>. The average monthly temperature and precipitation data were analyzed to identify trends and patterns.

The analysis aimed to identify the most critical months during the dry season (typically from June to September) and the monsoon season (usually from November to February) so that their relationship and effect on the soil moisture index and vegetation could be studied. By pinpointing these critical periods, it was possible to better understand how temperature and precipitation variations impacted soil moisture and vegetation health, which was essential for developing strategies to optimize oil palm yields and manage the effects of climate variability in agriculture.

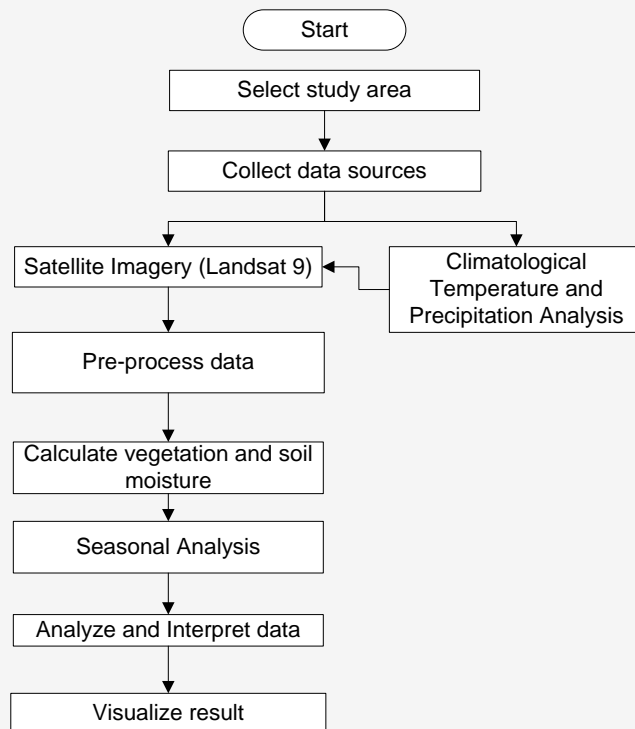


Figure 2: Seasonal monitoring and analysis of soil moisture

2.5 Vegetation and Soil Moisture Estimation

Landsat 9 images were selected based on climatology temperature-precipitation analysis for both dry and monsoon seasons, specifically for the months of July, August, December in 2021 and January in 2022. *Normalised Difference Vegetation Index (NDVI)* was employed in this research for evaluating vegetation health and its temporal variability under different climatic conditions. By using *NDVI*, it is possible to evaluate vegetation cover and detect stress conditions caused by seasonal variations. The index is particularly effective in distinguishing between healthy vegetation and areas of sparse vegetation or bare soil. Healthy vegetation reflects more NIR and less red light, resulting in higher *NDVI* values. The *NDVI* is calculated as shown in Equation 1:

$$NDVI = \frac{NIR - RED}{NIR + RED} \quad \text{Equation 1}$$

The *Soil Moisture Index (SMI)* is an essential indicator used to estimate the moisture content in the soil, which is crucial for assessing soil health and vegetation conditions. *SMI* provides valuable insights into soil-water availability and its impact on vegetation, particularly in agricultural areas such as oil palm plantations.

In this research, *SMI* was derived from remote sensing data by combining two critical indices: the *Normalised Difference Vegetation Index (NDVI)* and *Land Surface Temperature (LST)*. This combination allows for a more accurate assessment of soil moisture levels over large areas by integrating information about vegetation health and surface temperature. The *SMI* serves multiple purposes, including monitoring drought conditions, planning irrigation schedules, and evaluating overall agricultural productivity. In this research, the *SMI* was calculated based on the *LST* values, as shown in Equation 2:

$$SMI = \frac{LST_{max} - LST}{LST_{max} - LST_{min}} \quad \text{Equation 2}$$

For a given *NDVI*, the *Land Surface Temperature (LST)* represents the surface temperature of a pixel corresponding to a specific *NDVI* value, derived from remote sensing data. *LST* is a crucial parameter that reflects the thermal properties of the land surface and provides insights into soil moisture and vegetation conditions. The *LST* is calculated using the maximum and minimum land surface temperatures, which correspond to the highest and lowest temperatures recorded for a given *NDVI* value in the study area.

These values are critical for accurately representing the thermal environment of the land surface. The calculation of LST is based on Equation (3-7):

$$LST = \frac{T_b}{1 + \left(\alpha \frac{T_b}{C_2} \right) \ln \varepsilon}$$

Equation 3

Where T_b in °C is a satellite brightness temperature as in Equation 4, α is the wavelength of emitted radiance = 10.8, $C_2 = 14,388$ and ε is emissivity of the surface as in Equation 5:

$$T_b = \frac{K_2}{\ln \left(\frac{K_1}{L_\lambda} + 1 \right)} - 273.15$$

Equation 4

$$\varepsilon = 0.04P_v + 0.986$$

Equation 5

K_1 is sensor dependent calibration constant 1 (774.8853) and K_2 is sensor dependent calibration constant 2 (1321.0789), L_λ is Top of Atmosphere (TOA) spectral radiance as in Equation 6, P_v and CV is correction value for Landsat Images = 0.986.

$$L_\lambda = M_L Q_{cal} + A_L$$

Equation 6

Where:

- M_L : Radiance multiplicative scaling factor (gain) from metadata (0.0003342)
- A_L : Radiance additive scaling factor (offset) from metadata (0.1).
- Q_{cal} : Digital number (DN)

P_v in Equation 7 stands for vegetation proportion, which is the fraction or percentage of vegetation cover in each area, typically at the pixel level in remote sensing analysis. The formula of P_v as in Equation 7:

$$P_v = \left(\frac{NDVI - NDVI_{min}}{NDVI_{max} - NDVI_{min}} \right)^2$$

Equation 7

3. Result and Discussion

3.1 Climatology Temperature-Precipitation Analysis

Temperature and precipitation data were collected from the Climate Engine website, covering the period from 2014 to 2022, which encompasses a total of 9 years. After collecting the data, it was plotted to provide a clearer and more comprehensive graphical representation. Figure 3 illustrates the climate data plot over this 9-year period. The plot shows the variations and trends in temperature and precipitation over time. The temperature data reveal patterns of seasonal changes, highlighting periods of warmer and cooler temperatures. Meanwhile, the precipitation data depict fluctuations in rainfall, including periods of high and low precipitation. These trends help in understanding the overall climate behavior and identifying any significant anomalies or changes over the study period. To analyze the temperature and precipitation trends specifically during the monsoon, the data were divided into two seasons: the dry season and the monsoon season. This division allows for a more focused analysis of how climatic conditions vary between these two distinct periods. The analysis reveals a generally inverse relationship between precipitation and temperature.

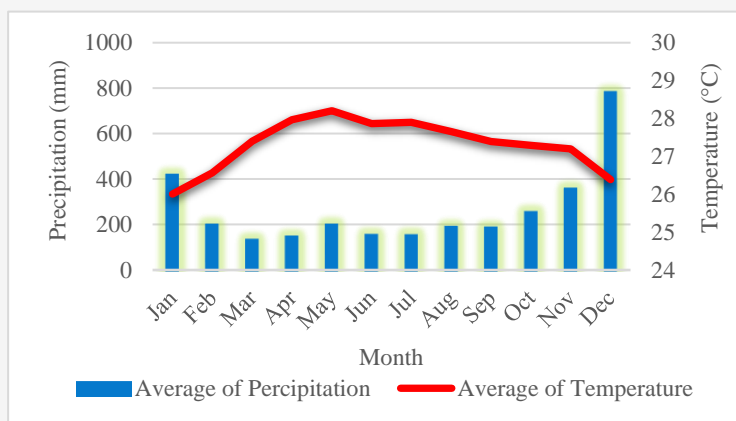


Figure 3: Average Precipitation and Temperature Trends from 2014 to 2022

For instance, the months of December and January, which experience high precipitation, correspond to lower average temperatures. This trend suggests that during periods of high precipitation, temperatures tend to drop, likely due to increased cloud cover and reduced solar radiation. Conversely, during the dry season from June to August, precipitation decreases significantly while temperatures remain relatively high, indicating reduced cloud cover and increased solar radiation. The data indicates a strong influence of the monsoon season, particularly in December and January, when high precipitation levels are observed. This is characteristic of tropical regions where monsoon rains significantly impact monthly precipitation patterns. In contrast, the dry season from June to August is marked by low precipitation and relatively high temperatures, suggesting potential water stress for crops during this period. This lack of rainfall and high temperatures likely lead to increased evaporation rates and reduced soil moisture, impacting crop health and growth.

To further investigate valuable insights into the seasonal impact on vegetation and soil moisture data, specific months were selected for detailed analysis. July and August, identified as the driest months, were chosen to understand the effects of minimal precipitation and higher temperatures on vegetation and soil moisture. In contrast, December, and January, recognized as the wettest months, were selected to analyze the influence of high precipitation and lower temperatures on these parameters. By comparing these distinct seasonal conditions, the study aimed to gain a comprehensive understanding of how varying climatic conditions affect vegetation health and soil moisture levels throughout the year.

3.2 Normalised Difference Vegetation Index (NDVI) Seasonal Analysis

The Normalised Difference Vegetation Index (NDVI) was classified as three levels: Level 1 (≤ 0.75), Level 2 (≤ 0.85), and Level 3 (≤ 1). January and December were chosen to study the impact of the monsoon season, which represents the wettest months, while July and August were chosen to evaluate the impact of the dry season, which represents the driest months. Blocks B36 and 37 (see Table 2 and 3) exhibit strong vegetation health during the dry and transitional months, with most of their areas classified under Level 3 NDVI, reflecting high vegetation health. In July, Block B36 shows 78.08% of its area at Level 3, while Block 37 records 72.19%. Vegetation health improves further in August, with Level 3 areas increasing to 67.94% in Block B36 and 87.54% in Block 37. Both blocks peak in December, with Block B36 and Block 37 having 81.79% and 90.32% of their areas, respectively, classified as Level 3. The absence of Level 1 in both blocks during these months highlights their strong vegetation resilience and response to favorable conditions, particularly during the monsoon transition. In January, during the wet season, vegetation health declines in both blocks. In Block B36, Level 3 areas drop sharply to 2.90%, with Level 2 dominating at 90.11%. Similarly, Block B37 sees Level 3 areas reduced to 22.36%, while Level 2 increases significantly to 77.31%. Both blocks also exhibit small portions of Level 1 areas for the first time, with 6.99% in Block B36 and 0.33% in Block B37. This decline in vegetation health during the wettest month suggests environmental stressors like waterlogging or reduced sunlight may have impacted vegetation in both blocks, marking a clear contrast to their strong performance earlier in the year.

Table 2: Number of pixels and percentage of NDVI for each level in Block B36






Block	July	August	December	January								
B36 												
	Level	No of pixel	%	Level	No of pixel	%	Level	No of pixel	%	Level	No of pixel	%
	1	0	0.00	1	0	0.00	1	53	6.99	1	0	0.00
	2	163	21.39	2	243	32.06	2	138	18.21	2	683	90.11
3	595	78.08	3	515	67.94	3	620	81.79	3	22	2.90	

Table 3: Number of pixels and percentage of NDVI for each level in Block B37








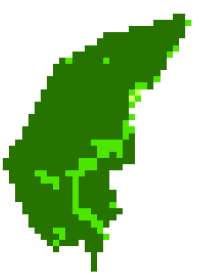
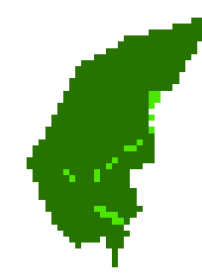
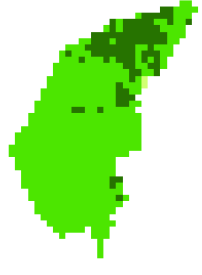
Block	July	August	December	January								
B37 												
	Level	No of pixel	%	Level	No of pixel	%	Level	No of pixel	%	Level	No of pixel	%
	1	0	0.00	1	0	0.00	1	0	0.00	1	3	0.33
	2	250	27.81	2	112	12.46	2	87	9.68	2	695	77.31
3	649	72.19	3	787	87.54	3	812	90.32	3	201	22.36	



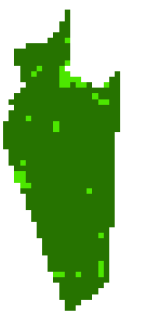

Table 4: Number of pixels and percentage of NDVI for each level in Block 38

Block	July	August	December	January								
B38 												
	Level	No of pixel	%	Level	No of pixel	%	Level	No of pixel	%	Level	No of pixel	%
	1	2	0.35	1	2	0.35	1	0	0.00	1	2	0.35
	2	124	21.91	2	63	11.13	2	24	4.24	2	469	82.86
3	440	77.74	3	501	88.52	3	542	95.76	3	95	16.78	

Block B38 in Table 4 shows high vegetation health in most months, with Level 3 *NDVI* dominating July, August, and December. In July, 77.74% of the block is classified as Level 3, and 21.91% falls under Level 2, leaving only a negligible portion in Level 1 (0.35%). Similarly, in August, Level 3 increases to 88.52%, with Level 2 decreasing slightly to 11.13%. By December, Level 3 reaches its peak at 95.76%, while Level 2 decreases further to 4.24%, indicating optimal vegetation health during this period. However, in January, vegetation health declines significantly, with Level 3 dropping to 16.78% and Level 2 becoming dominant at 82.86%. A small portion of the block, 0.35%, falls under Level 1, reflecting a minor decline in vegetation health during the wet season. Block B39 in Table 5 also exhibits strong vegetation health during July, August, and

December, with a dominance of Level 3 *NDVI*. In July, Level 3 accounts for 62.19%, and Level 2 covers 37.81%, with no areas classified as Level 1. Vegetation health improves further in August, with Level 3 increasing to 86.58% and Level 2 decreasing to 13.42%. By December, Level 3 reaches its maximum at 94.66%, with Level 2 covering only 5.34%. However, in January, vegetation health declines notably as Level 3 drops to 2.89%, and Level 2 becomes dominant at 90.04%. Additionally, a small portion of Level 1 emerges, accounting for 7.07%, indicating a greater impact of the wet season on this block compared to the others. Both Blocks 38 and 39 show strong vegetation health during the dry and transitional months, with high percentages of Level 3 *NDVI* in July, August, and December, reflecting favorable conditions.

Table 5: Number of pixels and percentage of NDVI for each level in Block 39

Block	July			August			December			January		
B39												
	Level	No of pixel	%	Level	No of pixel	%	Level	No of pixel	%	Level	No of pixel	%
	1	0	0.00	1	0	0.00	1	0	0.00	1	49	7.07
	2	262	37.81	2	93	13.42	2	37	5.34	2	624	90.04
3	431	62.19	3	600	86.58	3	656	94.66	3	20	2.89	

However, during the wet season in January, vegetation health declines in both blocks, as Level 3 areas decrease dramatically, and Level 2 becomes dominant. While wet season conditions usually lead to higher *NDVI* values, the increase in cloud cover, heavy rainfall, runoff, waterlogging, and lower temperatures in January all contribute to the unexpected drop in *NDVI*, though the values remain within a healthy range (0.7 to 0.85). Block B39 is particularly affected, with a more significant emergence of Level 1 areas (7.07%) compared to Block B38 (0.35%).

3.3 Soil Moisture Index (SMI) Seasonal Analysis

The *Soil Moisture Index (SMI)* was divided into five levels: Level 1 (≤ 0.35), Level 2 (≤ 0.5), Level 3 (≤ 0.65), Level 4 (≤ 0.8) and Level 5 (≤ 0.95). January and December were selected to analyze the impact of the monsoon season, representing the wettest months, while July and August were chosen to assess the impact of the dry season, representing the driest months. During the wettest months, soil moisture levels in Block B36 are predominantly classified as Level 4 and Level 5 in December, indicating higher moisture content. In contrast, January sees a significant decrease in *SMI*, with the value categorized under Level 2, as shown in Table 6. This decline is likely due to a combination of reduced rainfall, lower runoff, and stable evapotranspiration, resulting in the soil retaining less moisture. December exhibits a more even distribution, with 50.07% of the area classified under Level 4 and 49.93% under Level 5, reflecting the substantial impact of the monsoon season in increasing soil moisture. Conversely, during the driest months (July

and August), the *SMI* is entirely classified as Level 2 in July, underscoring the significant effect of the dry season in reducing soil moisture content. A marked shift occurs in August, where the *SMI* is entirely within Level 4, indicating a recovery in moisture levels despite the dry season's influence.

The trends for Block 37 are similar to those observed in Block B36 as in Table 7. In July, the *SMI* is dominated by Level 2 with 100%. However, in August, there is a shift, with Level 3 at 10.29% and Level 4 dominating at 89.71%. By December, Level 4 is still prominent at 35.20%, but Level 5 takes over as the dominant level with 64.80%. In January 2022, a more varied distribution is observed, with Level 1 representing 5.26%, Level 2 at 94.74%, and Level 3 at 6.60%. These fluctuations reflect the seasonal changes impacting soil moisture levels in the plantation area.

In December, Block B38 exhibits high soil moisture levels, with 95.52% of the area at Level 5, reflecting substantial moisture due to the monsoon season (see Table 8). Similarly, Block B39 displays elevated soil moisture levels, with 42.31% of the area at Level 4 and 57.69% at Level 5, which dominates the region (see Table 9). In August, Block B38 displays a nearly even distribution of soil moisture between Level 3 (48.22%) and Level 4 (51.78%). In contrast, Block B39 is predominantly at Level 3, covering 68.45%, while Level 4 occupies 25.46%. These patterns in August are similar for both blocks. For both July and January, Blocks B38 and B39 show identical *SMI* patterns, with 100% of the areas at Level 2. In July, this indicates very low soil moisture due to minimal rainfall during the driest month. Despite

Table 6: Number of pixels and percentage of SMI for each level in Block B36


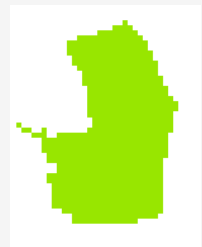

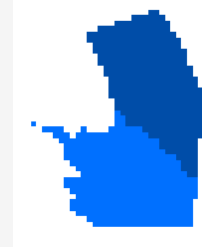
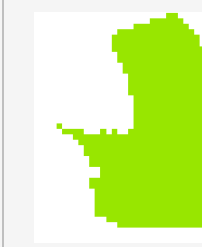
Block	July	August	December	January					
B36 									
	Level	No of pixel	%	Level	No of pixel	%	Level	No of pixel	%
	1	0	0.00	1	0	0.00	1	0	0.00
	2	721	100	2	0	0.00	2	0	0.00
	3	0	0.00	3	0	0.00	3	0	0.00
	4	0	0.00	4	718	100	4	359	50.07
	5	0	0.00	5	0	0.00	5	358	49.93
1	0	0.00	1	0	0.00	1	0	0.00	
2	716	100	2	0	0.00	2	0	0.00	
3	0	0.00	3	0	0.00	3	0	0.00	
4	0	0.00	4	718	100	4	359	50.07	
5	0	0.00	5	0	0.00	5	358	49.93	

Table 7: Number of pixels and percentage of SMI for each level in Block B37




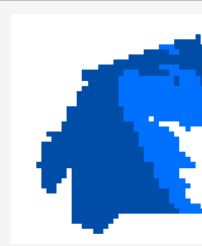
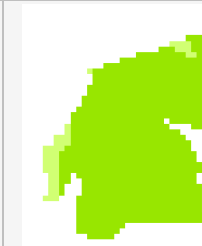
Block	July	August	December	January					
B37 									
	Level	No of pixel	%	Level	No of pixel	%	Level	No of pixel	%
	1	0	0.00	1	0	0.00	1	45	5.26
	2	860	100	2	0	0.00	2	811	94.74
	3	0	0.00	3	88	10.29	3	0	0.00
	4	0	0.00	4	767	89.71	4	302	35.20
	5	0	0.00	5	0	0.00	5	556	64.80
1	0	0.00	1	0	0.00	1	0	0.00	
2	860	100	2	0	0.00	2	0	0.00	
3	0	0.00	3	88	10.29	3	0	0.00	
4	0	0.00	4	767	89.71	4	302	35.20	
5	0	0.00	5	0	0.00	5	556	64.80	

Table 8: Number of pixels and percentage of SMI for each level in Block B38


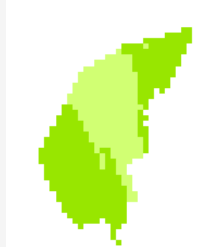


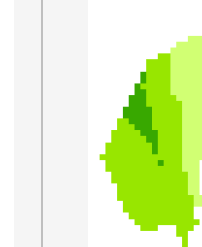





Block	July	August	December	January					
B38 									
	Level	No of pixel	%	Level	No of pixel	%	Level	No of pixel	%
	1	210	39.03	1	0	0.00	1	222	41.34
	2	328	60.97	2	0	0.00	2	279	51.96
	3	0	0.00	3	258	48.22	3	36	6.70
	4	0	0.00	4	277	51.78	4	0	0.00
	5	0	0.00	5	0	0.00	5	512	95.52
1	210	39.03	1	0	0.00	1	0	0.00	
2	328	60.97	2	0	0.00	2	0	0.00	
3	0	0.00	3	258	48.22	3	0	0.00	
4	0	0.00	4	277	51.78	4	24	4.48	
5	0	0.00	5	0	0.00	5	512	95.52	

Table 9: Number of pixels and percentage of SMI for each level in Block B39

Block	July	August	December	January								
B39 												
	Level	No of pixel	%	Level	No of pixel	%	Level	No of pixel	%	Level	No of pixel	%
	1	32	4.85	1	0	0.00	1	0	0.00	1	113	17.20
	2	628	95.15	2	40	6.10	2	0	0.00	2	544	82.80
	3	0	0.00	3	449	68.45	3	0	0.00	3	0	0.00
	4	0	0.00	4	167	25.46	4	278	42.31	4	0	0.00
5	0	0.00	5	0	0.00	5	379	57.69	5	0	0.00	

January being one of the wettest months, a sudden drop in soil moisture is observed. This drop is attributed to the combination of low rainfall, low runoff, and a stable evapotranspiration rate, consistent with the trends observed in Blocks B36 and B37 for January 2022. Based on the analysis of Blocks B36, B37, B38, and B39, seasonal variations have a significant impact on soil moisture content. During the wettest months, January and December, soil moisture levels are elevated across all blocks. In December, Block B36 predominantly shows Level 4 and Level 5 classifications, reflecting the substantial moisture from the monsoon season. A similar trend is observed in Blocks B37, B38, and B39, with Block B38 exhibiting 95.52% of the area at Level 5. However, in January, a significant decrease in moisture levels is noted, with Block B36 showing a shift to Level 2, likely due to reduced rainfall, lower runoff, and stable evapotranspiration rates.

In contrast, during the driest months, July and August, soil moisture content drops markedly. In July, most blocks, including Block B36, show moisture at Level 2, indicating the onset of dry conditions. By August, Blocks B36 and B37 exhibit a slight recovery, with the *SMI* predominantly at Level 4. In Blocks B38 and B39, moisture levels in August are split between Level 3 and Level 4, with Block B39 showing a dominance of Level 3 (68.45%) and Block B38 showing an almost equal distribution between Level 3 and Level 4. For both July and January, Blocks B38 and B39 follow identical patterns, with 100% of their areas at Level 2. These findings confirm that soil moisture levels are strongly influenced by seasonal variations, with higher moisture during the monsoon season and

lower moisture during the dry season. The *Soil Moisture Index (SMI)* provides a reliable indicator of these variations, making it a valuable tool for understanding soil conditions and predicting oil palm yield. The observed correlation between *SMI* and soil moisture suggests that incorporating *SMI* into predictive models could improve yield forecasts and enhance agricultural management strategies.

3.4 Heatmap Result Summary

The *NDVI* heatmaps in Figure 4 indicate significant seasonal variations in vegetation health across the monitored blocks (B36, B37, B38, and B39). In January, a noticeable increase in *NDVI* Level 1 values is observed, particularly in Blocks B36 and B39, with values of 7% and 7.1%, respectively, indicating poor vegetative health at the beginning of the monsoon season. This suggests that the vegetation in these areas is struggling due to water stress and reduced soil moisture following the dry months. In contrast, December shows a dramatic improvement, with most areas transitioning to *NDVI* Level 3, indicating high vegetative health. Blocks B38 and B39 exhibit the highest values at this level, reaching 96% and 95%, respectively, demonstrating the positive impact of the monsoon season in replenishing soil moisture and promoting plant growth. During the dry months of July and August, *NDVI* Level 2 dominates across the blocks, reflecting moderate vegetation health despite reduced precipitation. Block B39 maintains a significant proportion in Level 2, with values of 38 in July, suggesting that effective water management strategies may be in place to sustain plant growth.

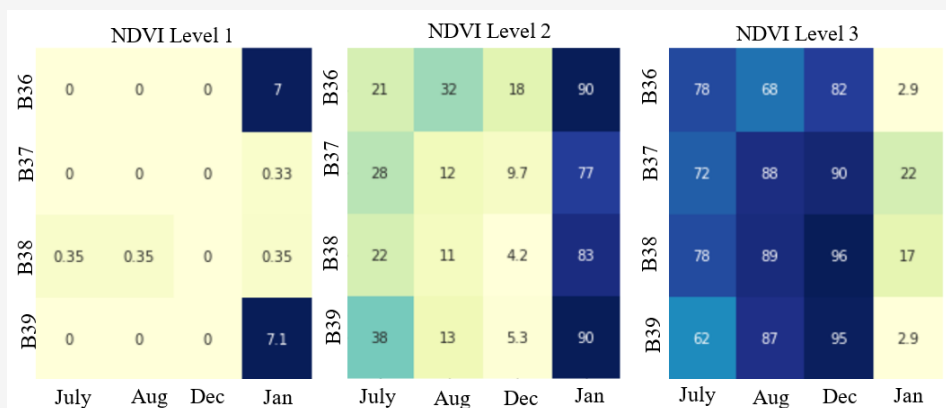


Figure 4: Heatmaps of Normalized Difference Vegetation Index (NDVI) levels across blocks

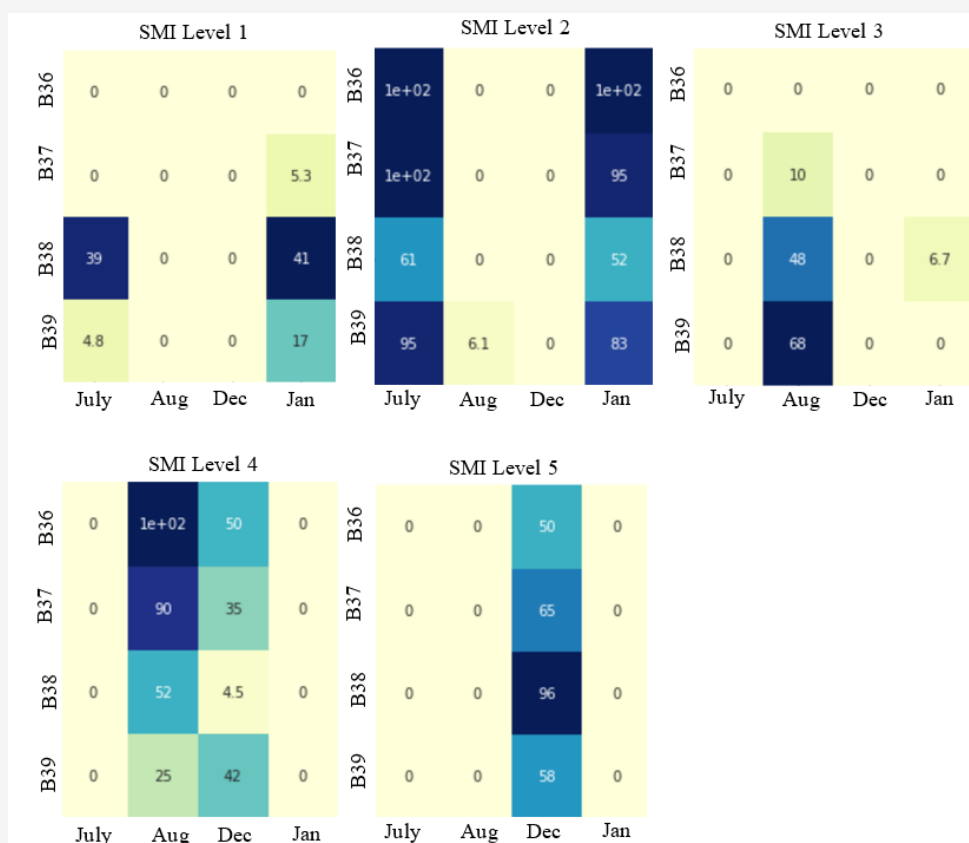


Figure 5: Heatmaps of Soil Moisture Index (SMI) levels across blocks

However, a steady increase in *NDVI* Level 3 from July to December highlights an improvement in vegetation health, with most areas benefiting from seasonal rainfall. In January, the shift from Level 3 to Level 2 across all blocks, especially in B37 and B38, suggests the seasonal effect of reduced moisture availability. These trends highlight the importance of seasonal rainfall in sustaining vegetation health and the potential role of irrigation measures in mitigating dry season stress.

Figure 5 shows that the analysis of the *SMI* heatmaps across plantation blocks B36 to B39. It shows that Level 1 *SMI* is mostly present in January and July. In January, it appears in more blocks, while in July, it is found in fewer areas. This suggests that these months have lower soil moisture, likely due to dry weather conditions with less rainfall and more evaporation. For Level 2 *SMI*, both January and July show an increase across all blocks, with January having the highest values.

This could be because of some rainfall or water retention in the soil during these months. On the other hand, August, and December show low values at Level 2, meaning that soil moisture in these months is either very low or shifts to higher levels.

In August, soil moisture increases to Level 3, especially in blocks B37, B38, and B39. August also shows a strong presence of Level 4 *SMI*, meaning soil moisture is quite high during this time. This might be due to rainfall or other factors that help the soil hold more water. December shows the highest soil moisture, with a significant presence at both Level 4 and Level 5 across all blocks. However, the moisture is highest at Level 5, meaning December has the most water in the soil. This could be due to the rainy season or lower evaporation rates, making it a good period for oil palm growth. Lastly, Level 5 *SMI* is only seen in December, while other months do not reach this level. This means December has the highest soil moisture, while other months have much lower levels. The changes in soil moisture throughout the year show the need for proper water management to support plant growth.

4. Conclusion

The objective of this study was to utilize remote sensing technology to monitor and analyze seasonal variations in soil moisture and vegetation health within oil palm plantations, providing insights for sustainable management. By integrating satellite data, the study explored the distribution of the *Soil Moisture Index (SMI)* and the *Normalised Difference Vegetation Index (NDVI)* across Blocks B36, B37, B38, and B39 during the wettest and driest months. The findings revealed clear seasonal patterns, with January and July showing the lowest moisture levels, predominantly at Level 1 *SMI*, indicating drier conditions. Despite the low soil moisture, *NDVI* values remained moderate to high, suggesting that effective water management practices helped sustain vegetation health during these dry months. In contrast, August showed an increase in moisture levels, with a strong presence at Levels 3 and 4 *SMI*, leading to improved vegetation health as indicated by higher *NDVI* values. December recorded the highest soil moisture, with significant dominance at Level 5 *SMI*, confirming it as the wettest period of the year. This increase in soil moisture corresponded with higher *NDVI* values, indicating optimal vegetation conditions. These results highlight the seasonal fluctuations in soil moisture and vegetation health across the plantation, emphasizing the importance of monitoring these parameters to optimize water management strategies. The study findings suggest that December provides the most favorable conditions for oil palm growth, while the drier

months of January and July may require targeted interventions to maintain soil moisture and vegetation health. However, the absence of irrigation data presents a limitation, as it may have contributed to inconsistencies observed in *SMI* and *NDVI* values across different months. Future research should incorporate irrigation data to better understand its impact on soil moisture distribution and vegetation health. Overall, this study demonstrates the effectiveness of using *SMI* and *NDVI* as valuable parameters for assessing soil moisture dynamics and vegetation health, highlighting the potential of remote sensing technologies in supporting sustainable oil palm plantation management.

Acknowledgement

This research article was financially supported by Universiti Teknologi MARA and Institute of Postgraduate Studies UiTM. The authors would like to thank School of Electrical Engineering, College of Engineering, Universiti Teknologi MARA, Cawangan Terengganu, Kampus Dungun and Shah Alam, Selangor for their valuable support.

References

- [1] Sishodia, R. P., Ray, R. L. and Singh, S. K., (2020). Applications of Remote Sensing in Precision Agriculture: A Review. *Remote Sens (Basel)*, Vol. 12(9), 1-31, <https://doi.org/10.3390/rs12193136>.
- [2] Patel, R. and Maitreya, B., (2022). A Review-Applications of Remote Sensing in the Agriculture. *International Journal of Research and Analytical Reviews (IJRAR)*, Vol. 9(2), 100-106. <https://www.ijrar.org/papers/IJAR22B1484.pdf>.
- [3] Maram, B. R., Vijayreddy, D. and Reddy, M. B., (2023). Recent Applications of Remote Sensing in Agriculture-A Review. *Journal of Agriculture Biotechnology & Applied Sciences*, Vol. 1(1), 28-35, <https://doi.org/10.5281/zenodo.8216660>.
- [4] Preedapirom, P., Robert, O., Onchang, R., and Jeefoo, P. (2024). Drought Monitoring Using MODIS Satellite-Based Data in Kamphaeng Phet Province, Thailand. *International Journal of Geoinformatics*, Vol. 20(1), 1–11. <https://doi.org/10.52939/ijg.v20i1.3019>.
- [5] Youssef, N., Gad, M., Elmoustafa, A., & Elleithy, D. (2023). Improving the Estimation of Soil Moisture in Semi-Arid Regions Using Data from Different Remote Sensing Techniques. *International Journal of Geoinformatics*, 19(8), 42–53. <https://doi.org/10.52939/ijg.v19i8.2781>

- [6] Namwong, C., Suwanpravit, C., Shahnawaz, S., and Wongpornchai, P. (2023). Assessing the Relationship between Forest Proportion, Soil Moisture Index and Net Primary Productivity in Pa Sak Ngam, Chiang Mai Province, Thailand. *International Journal of Geoinformatics*, Vol. 19(2), 25–38. <https://doi.org/10.52939/ijg.v19i2.2563>.
- [7] Cahyono, B. E., Putri, P. O., Subekti, A., Nugroho, A. T. and Nishi, K., (2022). Analysis of Soil Moisture as an Indicator of Land Quality Using Vegetation Index (SAVI and NDMI) Retrieved from Remote Sensing Data in Jember-Indonesia. *AIP Conference Proceedings, American Institute of Physics Inc.*, Vol. 2391(1). <https://doi.org/10.1063/5.0078761>.
- [8] Samanta, S. (2024). Identification of Agricultural Drought through Vegetation Health Analysis at Erap Station under the Markham Valley of Papua New Guinea. *International Journal of Geoinformatics*, Vol. 20(11), 106–115. <https://doi.org/10.52939/ijg.v20i11.3691>.
- [9] Zhao, H., Di, L., Sun, Z., Hao, P., Yu, E., Zhang, C. and Lin, L., (2021). Impacts of Soil Moisture on Crop Health: A Remote Sensing Perspective. *International Conference on Agro-Geoinformatics, Agro-Geoinformatics, Institute of Electrical and Electronics Engineers Inc*, 1-4. <https://doi.org/10.1109/Agro-Geoinformatics50104.2021.9530318>.
- [10] Qu, T., Li, Y., Zhao, Q., Yin, Y., Wang, Y., Li, F. and Zhang, W., (2024). Drone-Based Multispectral Remote Sensing Inversion for Typical Crop Soil Moisture under Dry Farming Conditions. *Agriculture (Switzerland)*, Vol. 14(3). <https://doi.org/10.3390/agriculture14030484>.
- [11] Gajbhiye, M., Agrawal, K. K., Jha, A. K., Kumar, N. and Raghuvanshi, M., (2023). Crop Health Monitoring through Remote Sensing: A Review. *International Journal of Environment and Climate Change*, Vol. 13(10), 2581-2589. <https://doi.org/10.9734/ijec/2023/v13i102924>.
- [12] Vlachopoulos, O., Leblon, B., Wang, J., Haddadi, A., Larocque, A. and Patterson, G., (2022). Evaluation of Crop Health Status with UAS Multispectral Imagery. *IEEE Journal of Selected Topics in Applied Earth Observations and Remote Sensing*, Vol. 15, 297-308, <https://doi.org/10.1109/JSTARS.2021.3132228>
- [13] Meena, S. V., Dhaka, V. S. and Sinwar, D., (2020). Exploring the Role of Vegetation Indices in Plant Diseases Identification. *International Conference on Parallel, Distributed and Grid Computing, Institute of Electrical and Electronics Engineers Inc*, 372–377. <https://doi.org/10.1109/PDGC50313.2020.9315814>.
- [14] Khan, N., Kamaruddin, M.A., Ullah Sheikh, U., Zawawi, M.H., Yusup, Y., Bakht, M.P. and Mohamed Noor, N., (2022). Prediction of Oil Palm Yield Using Machine Learning in the Perspective of Fluctuating Weather and Soil Moisture Conditions: Evaluation of a Generic Workflow. *Plants*, Vol. 11(13), <https://doi.org/10.3390/plants11131697>.
- [15] Yu, S., Mo, Q., Chen, Y., Li, Y., Li, Y., Zou, B., Xia, H., Jun, W., Li, Z. and Wang, F., (2020). Effects of Seasonal Precipitation Change on Soil Respiration Processes in A Seasonally Dry Tropical Forest. *Ecology and Evolution*, Vol. 10(1), 467–479. <https://doi.org/10.1002/ece3.5912>.
- [16] Feng, Y., Wang, H., Liu, W. and Sun, F., (2023). Global Soil Moisture-Climate Interactions during the Peak Growing Season. *Journal of Climate*, Vol. 36(4), 1187-1196. <http://doi.org/10.1175/JCLI-D-22-0161.1>.
- [17] Van Der Werff, H., Ettema, J., Sampatirao, A. and Hewson, R., (2022). How Weather Affects over Time the Repeatability of Spectral Indices Used for Geological Remote Sensing. *Remote Sensing*, Vol. 14(24), <http://dx.doi.org/10.3390/rs14246303>.
- [18] Cui, X., Xu, G., He, X. and Luo, D., (2022). Influences of Seasonal Soil Moisture and Temperature on Vegetation Phenology in the Qilian Mountains. *Remote Sensing*, Vol. 14(15), <http://dx.doi.org/10.3390/rs14153645>.
- [19] Sehler, R., Li, J., Reager, J. and Ye, H., (2019). Investigating Relationship Between Soil Moisture and Precipitation Globally Using Remote Sensing Observations. *Journal of Contemporary Water Research & Education*, Vol. 168(1), 106-118. <http://dx.doi.org/10.1111/j.1936-704x.2019.03324.x>.
- [20] Weidan, W., Li, S., Zhiyuan, P., Yuanyuan, C. and Mo, D., (2021). Comparison of TVDI and Soil Moisture Response Based on Various Vegetation Indices. *International Conference on Agro-Geoinformatics, Agro-Geoinformatics, Institute of Electrical and Electronics Engineers Inc*, 1-5. <http://dx.doi.org/10.1109/Agro-Geoinformatics50104.2021.9530348>.
- [21] Irenasari, A. H. and Soemarno, S., (2022). Soil Moisture Assessment Using Soil Moisture Index (SMI) Method at the Bangelan Coffee Plantation, Malang Regency, East Java. *Jurnal Tanah dan Sumberdaya Lahan*, Vol. 9(1)1, 1-

- 12, <http://dx.doi.org/10.21776/ub.jtsl.2022.009.1.1>.
- [22] Marzukhi, F. and Rosnan, N. N. R. and Said, M. A. M., (2020). Healthiness of Oil Palm Plantation Towards Sustainability of Environment. *Malaysian Journal of Sustainable Environment*, Vol. 7(1), <http://dx.doi.org/10.24191/myse.v7i1.8921>.
- [23] Saha, A., Patil, M., Goyal, V. C. and Rathore, D. S., (2018). Assessment and Impact of Soil Moisture Index in Agricultural Drought Estimation Using Remote Sensing and GIS Techniques. *Proceedings 2019*, Vol. 7(1). <http://dx.doi.org/10.3390/ecws-3-05802>.
- [24] Zauhairah, S. F., Barus, B., Wahjunie, E. D., Tjahjono, B. and Murtadho, A., (2022). Determination of Optimal Soil Moisture Mapping in Oil Palm Plantation Land (Case Study: Cikasungka Plantation, PT Perkebunan Nusantara VIII, Cimulang, Bogor). *Jurnal Tanah dan Sumberdaya Lahan*, Vol. 9(2), 447–456. <http://dx.doi.org/10.21776/ub.jtsl.2022.009.2.26>.
- [25] Potić, I., Bugarski, M. and Matić-Varenica, J., (2017). Soil Moisture Determination Using Remote Sensing Data for the Property Protection and Increase of Agriculture Production. *Worldbank Conference on Land and Poverty, The World Bank, Washington DC*.
- [26] Vijayanand, V. and Dhanya, M., (2024). Analysis of the Relationship between Heatwaves with Vegetation and Soil Moisture. *International Conference on Computing for Sustainable Global Development (INDIACom)*, 679–684. <https://doi.org/10.23919/INDIACom61295.2024.10499132>.
- [27] Hamim, M., Aziz, A., Khairunniza Bejo, S., Hashim, F., Ramli, N. H. and Ahmad, D., (2019). Evaluations of Soil Resistivity in Relation to Basal Stem Rot Incidences Using Soil Moisture Sensor. *Pertanika Journal of Science & Technology*, Vol. 27(S1), 225-234.
- [28] Waite, P.A., Schuldt, B., Mathias Link, R., Breidenbach, N., Triadiati, T., Hennings, N., Saad, A. and Leuschner, C., (2019). Soil Moisture Regime and Palm Height Influence Embolism Resistance in Oil Palm. *Oxford University Press*. <https://doi.org/10.1093/treephys/tpz061>.
- [29] Shashikant, V., Shariff, A. R. M., Wayayok, A., Kamal, M. R., Lee, Y. P. and Takeuchi, W., (2021). Vegetation Effects on Soil Moisture Retrieval from Water Cloud Model Using Palsar-2 for Oil Palm Trees. *Remote Sensing*, Vol. 13(20). <http://dx.doi.org/10.3390/rs13204023>.
- [30] Hermawan, B., Agustian, I., Herawati, R. and Gonggo Murcitra, B., (2021). Spatiotemporal Variability in Soil Water Content Profiles under Young and Mature Oil Palm Plantations in North Bengkulu Regency. *International Journal on Advanced Science Engineering Information Technology*, Vol. 11(1), 259-265, <http://dx.doi.org/10.18517/ijaseit.11.1.9432>.
- [31] Najihah, T. S., Ibrahim, M. H., Razak, A. A., Nulit, R. and Megat, P. E. W., (2019). Effects of Water Stress on the Growth, Physiology and Biochemical Properties of Oil Palm Seedlings. *AIMS Agriculture and Food*, Vol. 4(4), 854-868. <http://dx.doi.org/10.3934/agrfood.2019.4.854>.